Incorporation of P_2O_5 in a Na_2O-rich aluminoborosilicate glass

Sophie Achigar, Daniel Caurant, Elise Régnier, Odile Majérus, Thibault Charpentier

▶ **To cite this version:**

Sophie Achigar, Daniel Caurant, Elise Régnier, Odile Majérus, Thibault Charpentier. Incorporation of P_2O_5 in a Na_2O-rich aluminoborosilicate glass. Materials Letters, 2024, 377, pp.137283. 10.1016/j.matlet.2024.137283 . hal-04696542

HAL Id: hal-04696542
https://hal.science/hal-04696542v1

Submitted on 13 Sep 2024

HAL is a multi-disciplinary open access archive for the deposit and dissemination of scientific research documents, whether they are published or not. The documents may come from teaching and research institutions in France or abroad, or from public or private research centers.

L'archive ouverte pluridisciplinaire **HAL**, est destinée au dépôt et à la diffusion de documents scientifiques de niveau recherche, publiés ou non, émanant des établissements d'enseignement et de recherche français ou étrangers, des laboratoires publics ou privés.

Materials Letters Volume 377, 15 December 2024, 137283

https://doi.org/10.1016/j.matlet.2024.137283

Incorporation of P_2O_5 in a Na_2O-rich aluminoborosilicate glass

Sophie Achigar[a,b], Daniel Caurant[a,*], Elise Régnier[b], Odile Majérus[a], Thibault Charpentier[c]

[a]*Chimie ParisTech, PSL Research University, Centre National de la Recherche Scientifique (CNRS), Institut de Recherche de Chimie Paris (IRCP), 75005 Paris, France*

[b]*CEA, DES, ISEC, DPME, SEME, LFCM, Univ Montpellier, 30207 Marcoule, France*

[c]*Université Paris-Saclay, CEA, CNRS, NIMBE, 91191 Gif-sur-Yvette, France*

*Corresponding author. *E-mail address:* daniel.caurant@chimieparistech.psl.eu (Daniel Caurant)

Abstract

This work focuses on the effect of adding increasing amounts of P_2O_5 (0-10 mol%) on the microstructure and crystallization tendency of a Na_2O-rich aluminoborosilicate simplified nuclear glassy matrix obtained after melt quenching or controlled cooling from 1100°C. Above 2 mol% P_2O_5, phase separation followed by crystallization of Na_3PO_4 occurred, then followed by $NaCaPO_4$ and even $Na_4P_2O_7$ when P_2O_5 content reached 10 mol%. The Na_2O and CaO depletion induced in the residual glass by phosphate phases crystallization is responsible for an important increase of its glass transition temperature due to a significant increase of the silicate network polymerization as confirmed by ^{29}Si MAS NMR.

Keywords: P_2O_5 solubility, borosilicate glass, phosphate crystallization, ^{29}Si MAS NMR

1. Introduction

Dismantling nuclear facilities leads to radioactive waste which may have highly variable compositions. In a previous work, we focused on the waste coming from the dismantling operation of a French spent fuel reprocessing facility studying the ability of an alkali-rich (~ 33 mol% alkali oxides) glassy matrix belonging to the SiO_2-B_2O_3-Al_2O_3-Fe_2O_3-Na_2O-Li_2O-CaO system to solubilize simulated wastes containing P_2O_5, MoO_3 and ZrO_2 (abundant in the real waste) [1]. In this paper, to complete the previous study, we focused on the effect of phosphorus, and more precisely on the impact of adding increasing P_2O_5 amounts on the phase separation and crystallization tendency in the melt and during cooling of a simplified version of the alkali-rich glass previously investigated. For this, we synthesized quenched and slowly cooled samples belonging to the SiO_2-B_2O_3-Al_2O_3-Na_2O-CaO system derived from the previous glass composition, by adding increasing P_2O_5 amounts (0-10 mol%). The samples microstructure and the crystallization of phosphate phases were investigated using X-ray diffraction (XRD), scanning electron microscopy coupled with energy dispersive X-ray analysis (SEM-EDX) and ^{29}Si MAS NMR spectroscopy.

2. Experimental

A series of six peralkaline samples (Na/(B+Al) > 1) was prepared by adding increasing P_2O_5 amounts (0-10 mol%, in 2 mol% step) to the composition $50.6SiO_2$-$8.2B_2O_3$-$33.4Na_2O$-$6.1CaO$-$1.7Al_2O_3$ (mol%) from reagent grade SiO_2, H_3BO_3, Na_2CO_3, $CaCO_3$, Al_2O_3 and $NH_4H_2PO_4$ powders: the melting was performed in two times at 1100°C during 2 h in platinum crucibles, with an intermediate {casting + grinding} step to guarantee the glass homogeneity. To finish, the melt was cooled either rapidly (~10^4 °C.min^{-1}) between two brass plates (quenched samples) or slowly at 1°C.min^{-1} (slowly cooled samples). Above 10 mol% P_2O_5 a macroscopic phase separation occurred in the melt which justifies the upper limit chosen for

this study. SEM observations were performed with a FEG-SEM Zeiss Supra TM55 microscope. The chemical analysis of the quenched samples by EDX (Bruker AXS X-Flash Detector 4010) indicated that compositions were close to the target ones, even if boron cannot be quantified by this technique. Differential thermal analysis (DTA/TG STA 449 Netzsch) was used to determine the glass transition temperature (T_g) of the quenched samples. The crystalline phases present in the samples were studied and identified by XRD (X'Pert PRO PANalytical diffractometer (CuK_α radiation, λ=0.15406 nm)). For several quenched samples, the structural evolution of the silicate network was followed by ^{29}Si MAS NMR (data were collected on a Bruker Avance II 300WB spectrometer with a magnetic field of 7 T using a Bruker 4 mm CPMAS at a spinning frequency of 12.5 kHz).

3. Results and discussion

Quenched samples containing less than 8 mol% P_2O_5 appeared transparent, while above this concentration they were opalescent or opaque, which agrees with the detection of heterogeneities by SEM above 6 mol% P_2O_5 (Fig.1a,b). Nevertheless, XRD put in evidence the crystallization of phosphate phases above 2 mol% P_2O_5, firstly only γ-Na_3PO_4 (sodium orthophosphate) from 4 mol% P_2O_5, followed by $NaCaPO_4$ (sodium-calcium orthophosphate) and $Na_4P_2O_7$ (sodium pyrophosphate) for the highest P_2O_5 content (Figs.1a,b and 2a). In comparison, the slowly cooled samples all appeared opalescent or opaque, except the one without P_2O_5. A complex evolution of their microstructure - coupling phase separation (droplet like morphology) and subsequent crystallization - was observed by SEM above 2 mol% P_2O_5, with an increasing proportion of crystalline heterogeneities with P_2O_5 concentration identified by EDX and XRD (Figs.1c-f and 2b). Whereas only a weak crystallization of γ-Na_3PO_4 was detected for the sample with 2 mol% P_2O_5 (dendritic crystals mainly grown from sample surface, Fig.1c), an increasing crystallization of γ-Na_3PO_4 and $NaCaPO_4$ was then put in evidence, followed by $Na_4P_2O_7$ and cristobalite with 10 mol% P_2O_5 (Fig.1d-f). All these results

clearly show the high tendency of phosphorus above 2 mol% P_2O_5 to separate from the borosilicate network during slow cooling and are in accordance with the ones obtained in our previous work on a more complex system which showed that the crystallization of phosphate phases ($NaLi_2PO_4$, $NaCaPO_4$) also appeared above 2 mol% P_2O_5 [1]. This crystallization tendency of phosphate phases above several mol% P_2O_5 is also in agreement with the results reported by Stone-Weiss et al. on peralkaline Na_2O-rich borosilicate glasses even if in this study the amount of B_2O_3 was significantly higher than in the present work [2]. This crystallization tendency is in accordance with structural results reported in literature showing that phosphorus is mainly present as isolated orthophosphate and pyrophosphate entities in silicate glasses rich in alkali and alkaline-earth oxides [3,4]. Such isolated monomeric and dimeric phosphate entities would easily agglomerate in the supercooled melt during cooling, leading respectively to orthophosphate and pyrophosphate crystallization. The significant crystallization of sodium pyrophosphate (constituted of dimeric $P_2O_7^{4-}$ entities) for the highest P_2O_5 content (10 mol%, Fig.2) can be explained by the progressive decrease with P_2O_5 content of the total amount of $Na^+ + Ca^{2+}$ cations available to compensate new isolated monomeric entities PO_4^{3-} (each PO_4^{3-} entity needs 3 Na^+ or 1 Na^+ + 1 Ca^{2+} cations for charge compensation, i.e. 3 positive charges per P atom). Indeed, as shown in Fig.3a, when P_2O_5 concentration reaches 10 mol% the amount of $Na^+ + Ca^{2+}$ cations that would be needed to compensate all PO_4^{3-} entities (if all phosphorus were present as PO_4^{3-} units) becomes higher than the total $Na^+ + Ca^{2+}$ cations amount available in the sample. This could thus explain the formation of pyrophosphate crystals rather than only orthophosphate ones for the highest P_2O_5 content to reduce the amount of positive charge needed per phosphorus atom for charge compensation (each $P_2O_7^{4-}$ entity needs 4 Na^+ cations for local charge compensation, i.e. 2 positive charges per P atom), and the macroscopic separation in the melt of a highly crystallized phase containing a high proportion of $Na_4P_2O_7$ when 12 mol% P_2O_5 is added to the composition (XRD pattern not shown).

EDX analysis of the slowly cooled samples showed that phosphate phases crystallization induced an important Na_2O+CaO depletion in the residual glass surrounding the crystals, accompanied by a significant SiO_2 and B_2O_3 enrichment whereas no more than 1 mol% P_2O_5 remained in the glass (Fig.3b). Assuming that the evolution of the residual glass composition was similar for quenched and slowly cooled samples, both the increase of the proportion of glass formers (SiO_2, B_2O_3) and the decrease of the proportion of glass modifiers (Na_2O, CaO) in the residual glass could explain the increase of T_g with P_2O_5 content for the quenched samples (~100°C, Fig.3c). The global increase of the fraction of BO_4 units (Fig.3a) also contributes to the increase of the reticulation of the glassy network. Moreover, the increase of the slope of T_g evolution observed above 4 mol% P_2O_5 could be correlated with the change of the evolution of SiO_2 and B_2O_3 (slope increase), Na_2O and CaO (slope decrease) concentrations in the residual glass above 4 mol% P_2O_5 (Fig.3b) due to phosphate phases crystallization (Fig.2a). A similar T_g evolution was observed by Skerratt-Love et al. by adding increasing P_2O_5 contents in a sodium borosilicate glass [5]. In agreement with both the evolution of the residual glass composition (increase of the SiO_2/(Na_2O+CaO) concentration ratio), the increase of the proportion of BO_4^- entities and the increase of T_g with P_2O_5 content (Fig.3), a displacement towards more negative chemical shift values of the ^{29}Si MAS NMR spectra of the quenched samples was observed (Fig.4a), indicating an increase of the silicate network polymerization (increase of the proportion of bridging oxygen atoms (BO)) related to the increasing mobilization of Na^+ and Ca^{2+} cations to compensate the negative charge of phosphate entities in phosphate crystals (Fig.4b). Whereas the glass without phosphorus is significantly depolymerized as shown by the presence of both Q_3, Q_2 and Q_1 entities, an increasing contribution of Q_3 and Q_4 entities at the expense of Q_2 and Q_1 entities is put in evidence with P_2O_5 addition (Fig.4a). The highly depolymerized character of the glass without P_2O_5 is expected by calculating the average number N of NBOs formed per SiO_4 tetrahedra (N=1.34) by the amount of Na_2O+CaO available to act as modifiers (taking into account the BO_4^- and

AlO_4^- entities present in glass structure). The increase with P_2O_5 content of the reticulation of the glassy network (calculated as the proportion of BO in the residual glass) shown in Fig.3c agrees with the increase of T_g and ^{29}Si MAS NMR results.

It is interesting to notice that it is not the room temperature stable form of sodium orthophosphate α-Na_3PO_4 (tetragonal structure) that was identified by XRD in the quenched or slowly cooled samples (Fig.2a,b), but the metastable γ-Na_3PO_4 form (cubic structure, stable only above 320°C). The presence of this high-temperature crystalline form could be explained by the incorporation of calcium in the structure of the sodium orthophosphate crystals formed during cooling actually leading to $Na_{3-2x}Ca_xPO_4$ composition, as shown by EDX analysis for the slowly cooled samples (x~0.2-0.3). This partial Na/Ca substitution would stabilize the high temperature crystalline γ-form at room temperature. Indeed, by preparing $Na_{3-2x}Ca_xPO_4$ ceramic pellets (x=0-0.30) at 800-900°C, we confirmed that even when x=0.05, the γ-form was detected at the same time as the α-form and when $x \geq 0.15$, only the γ-form was present. However, using the same preparation method with x=0 (i.e. without calcium), only the α-form was present (the formation of the $NaCaPO_4$ phase was only detected from x=0.25 upwards). Nevertheless, this cannot be the only explanation for the crystallization of only γ-Na_3PO_4 in our samples because by removing CaO from the composition with 6 mol% P_2O_5, the crystallization of only γ-Na_3PO_4 was still detected after slow cooling (crystallization of γ-Na_3PO_4 was also observed by Skerratt-Love et al. in their sodium borosilicate glasses without CaO [5]). During crystallization, the partial substitution of a small amount of Si (coming from the glass composition) in the P site of Na_3PO_4 crystals could also stabilize the high temperature crystalline γ-form, as shown by Hopper et al. for lightly Si-doped $Na_{3(1+x)}P_{(1-3x)}Si_{3x}O_4$ ceramics [6]. Indeed, by EDX we detected the presence of a weak quantity of silicon (<1 mol% SiO_2) in the sodium orthophosphate crystals.

4. Conclusion

The microstructural and structural investigations of the quenched and slowly cooled P_2O_5-bearing Na-rich aluminoborosilicate samples presented in this study showed that above 2 mol% P_2O_5, phase separation followed by crystallization of γ-Na_3PO_4 occurred, then followed by $NaCaPO_4$ and even $Na_4P_2O_7$ when P_2O_5 content reached 10 mol%. The Na_2O+CaO depletion induced in the residual glass by phosphate phases crystallization is responsible for an important increase of T_g (~100°C) due to a significant increase of the silicate network polymerization as shown by ^{29}Si MAS NMR. Complementary studies by ^{31}P, ^{11}B, ^{27}Al and ^{23}Na MAS NMR and Raman spectroscopies will be presented in a forthcoming paper. The next step of this study will consist in determining the impact of these crystallized phases and of the polymerization of the residual glass on the long-term behavior (chemical durability) of the partially crystallized glasses.

Acknowledgments

This study was a part of the DEM&MELT project, which was a partnership between CEA, industrial partners (Orano, ECM Technologies), and ANDRA. This project was supported by the French government program titled “Programme d’Investissements d’Avenir (PIA)”, whose management was entrusted to ANDRA.

Figure 1

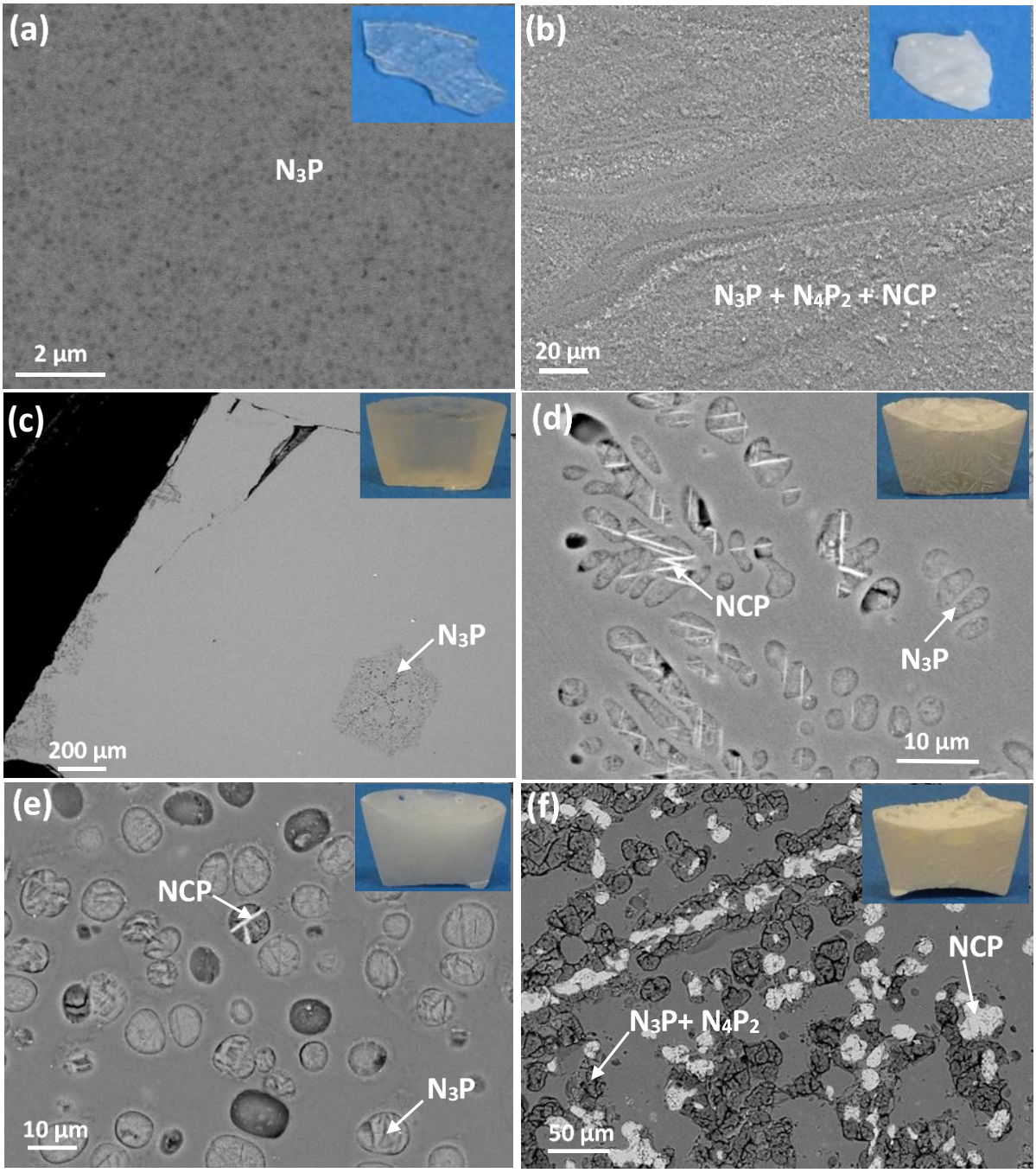

Figure 1. SEM images (backscattered electrons) of quenched samples with 8% (a) and 10% (b) P_2O_5 and slowly cooled samples with 2% (c), 4% (d), 6% (e) and 10% P_2O_5. N_3P (γ-Na_3PO_4), NCP ($NaCaPO_4$), N_4P_2 ($Na_4P_2O_7$). Macroscopic pictures of the samples are shown in inset.

Figure 2

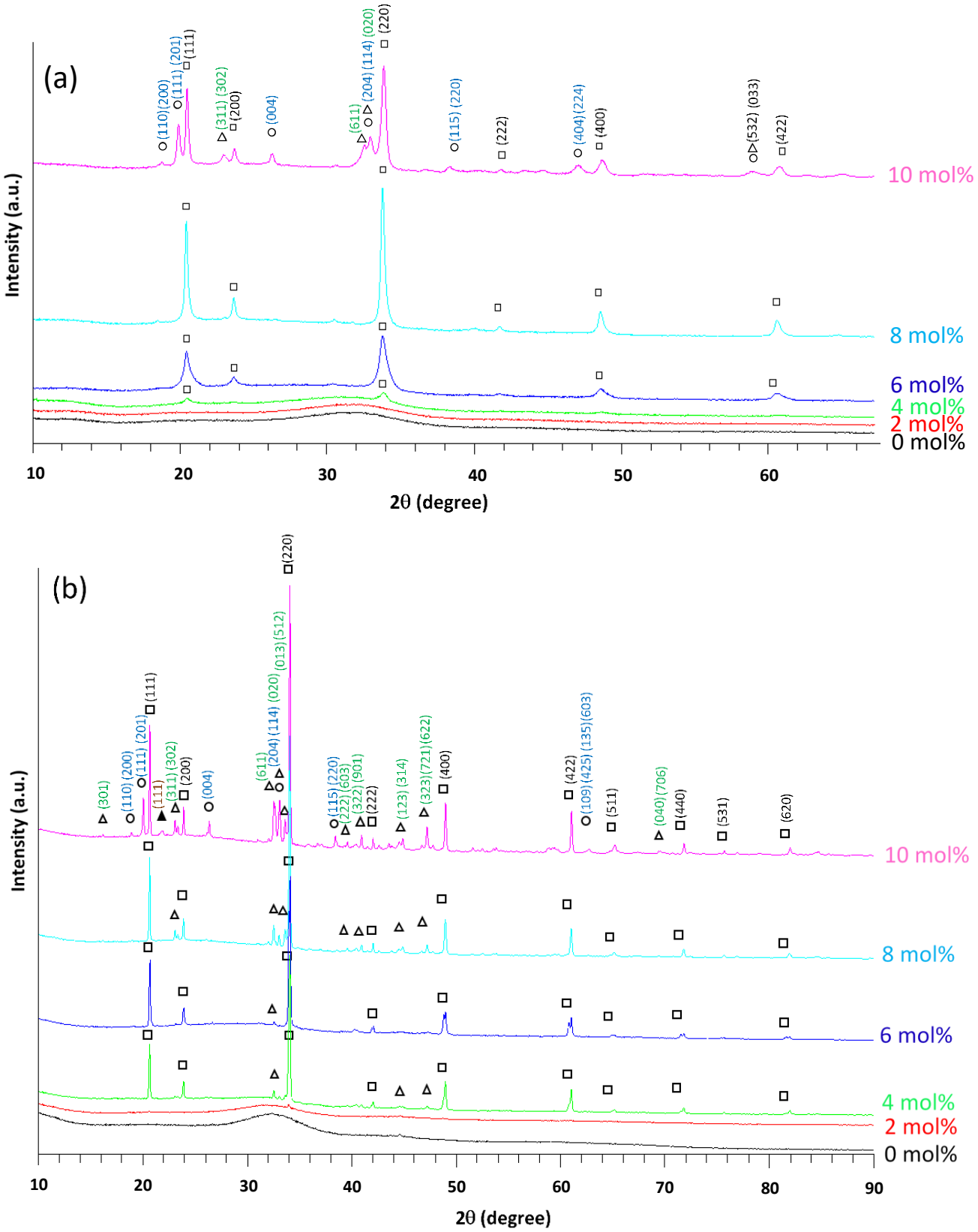

Figure 2. XRD patterns recorded at room temperature of the quenched (a) and slowly cooled (b) samples increasing P_2O_5 contents (0-10 mol%). □ (γ-Na_3PO_4 PDF#:00-031-1318), ○ ($Na_4P_2O_7$ PDF#:04-018-4331), △ ($NaCaPO_4$ PDF#:04-0016-6900), ▲ (SiO_2 cristobalite PDF#:04-013-9484).

Figure 3

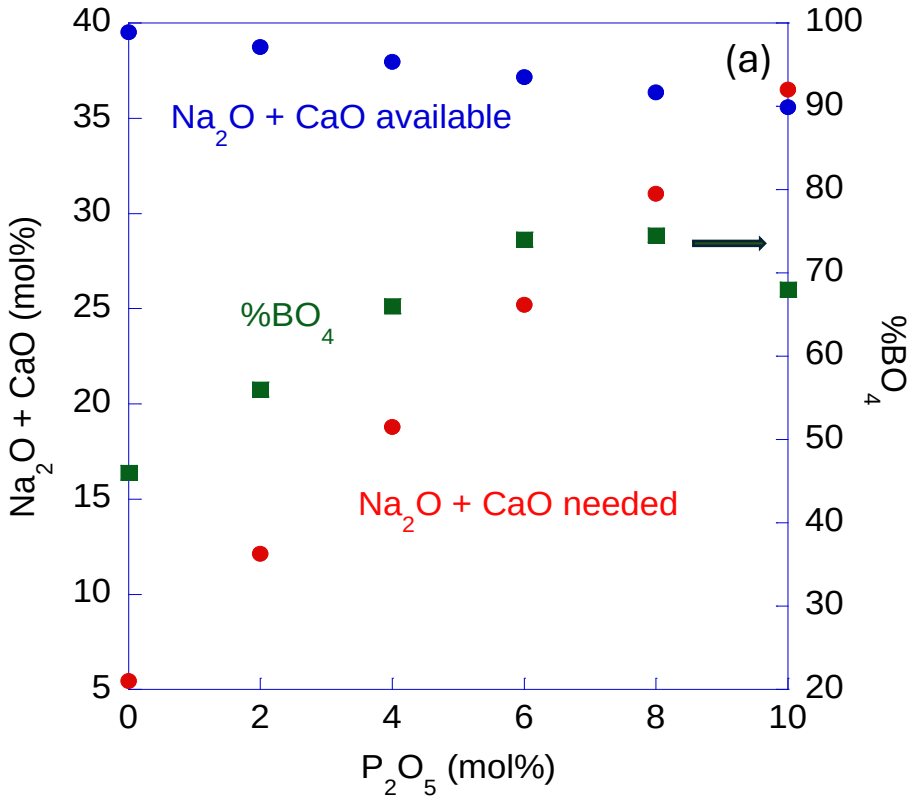
(a)
Na2O + CaO available
%BO4
Na2O + CaO needed
Na2O + CaO (mol%)
%BO4
P2O5 (mol%)
40
35
30
25
20
15
10
5
100
90
80
70
60
50
40
30
20
0
2
4
6
8
10

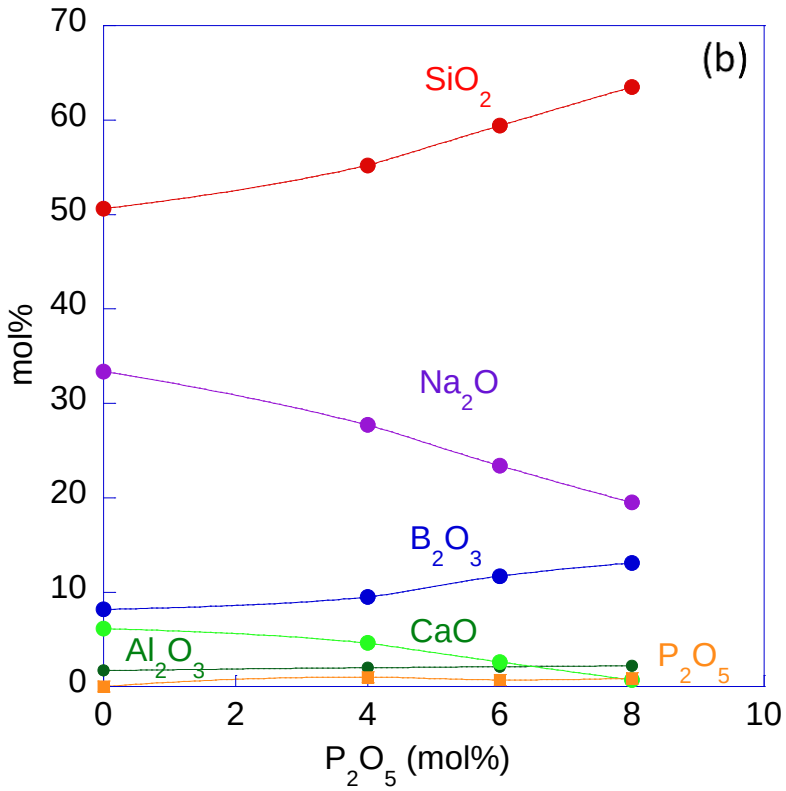
(b)
SiO2
Na2O
B2O3
CaO
Al2O3
P2O5
mol%
P2O5 (mol%)
70
60
50
40
30
20
10
0
0
2
4
6
8
10

Figure 3 (continue)

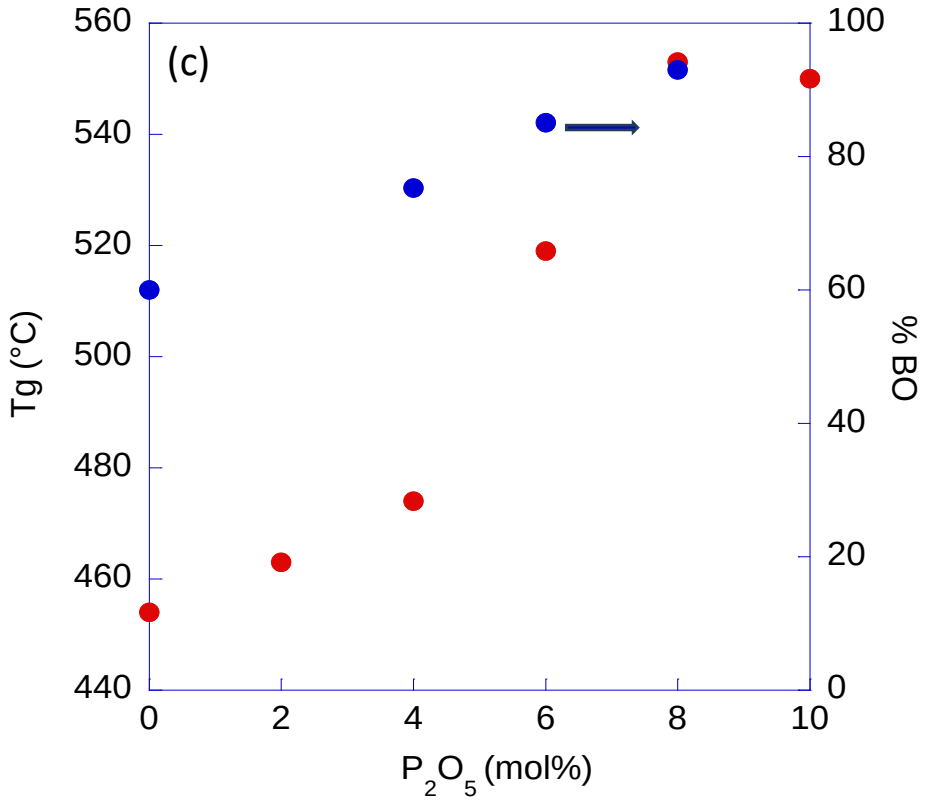

Figure 3. Evolution with P_2O_5 content : (a) of the Na_2O + CaO amount needed to compensate the negative charge of phosphate entities (if it is assumed that all phosphorus is present as orthophosphate entities) and available in the samples (taking into account the amount of Na^+ + Ca^{2+} ions needed to compensate the BO_4^- and AlO_4^- entities present in glass structure, according to ^{11}B and ^{27}Al MAS NMR results for the quenched samples not presented in this paper (The evolution of the relative proportion of BO_4^- entities deduced from ^{11}B MAS NMR is shown in the figure. Except for the sample with 10 mol% P_2O_5 for which a very small fraction of aluminum was detected in five-fold coordination by ^{27}Al MAS NMR, for all other samples aluminum is only present as AlO_4^- entities). (b) of the composition of the residual glass surrounding the crystalline phases for several slowly cooled samples (EDX analysis, B_2O_3 was estimated by difference to 100%). (c) of T_g for the quenched samples and of the percentage of bridging oxygen atoms (% BO) in the glassy phase (in blue) calculated from the residual glass composition (Fig.3b) and the relative proportion of BO_4^- entities (Fig.3a) assuming that all aluminum and phosphorus are present respectively as AlO_4^- and PO_4^{3-} entities in the glass. Lines in Fig.3b are guides for the eyes.

Figure 4

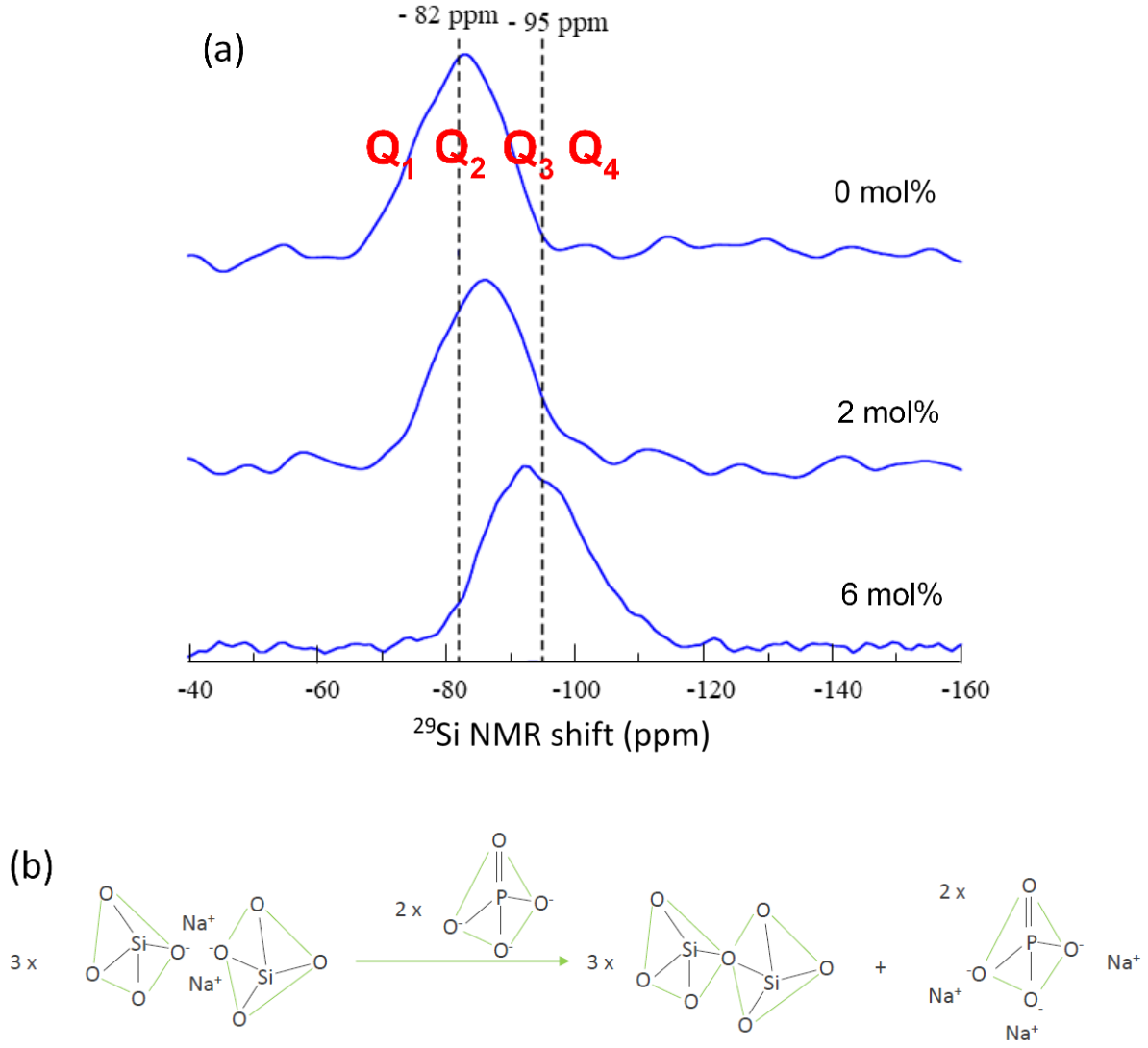

Figure 4. (a) Evolution of ^{29}Si MAS NMR spectra for several quenched samples with increasing P_2O_5 content. Q_1, Q_2, Q_3 and Q_4 indications correspond to the chemical shift range expected for Q_n entities (SiO_4 tetrahedral units with n bridging oxygens) in alkali silicate glasses. (b) Structural scheme showing the reticulating effect of the addition of P_2O_5 (here as PO_4^{3-} units present in the glass or in the crystals) on the silicate network (each PO_4^{3-} units added needs $3Na^+$ for charge compensation leading to the disappearance of 3 non-bridging oxygens).

References

[1] S. Achigar et al., J. Nucl. Mater. 544 (2021) 152731.

[2] N. Stone-Weiss et al., J. Phys. Chem. C 124 (2020) 17655.

[3] R. Dupree, et al., J. Non-Cryst. Solids. 106 (1988) 403.

[4] R. Mathew et al., Chem. Mater. 25 (2013) 1877.

[5] K.L. Skerratt-Love et al., J. Non-Cryst. Solids 600 (2023) 121999.

[6] A. Hooper et al. J. Solid State Chem. 24 (1978) 265.